Figure S1

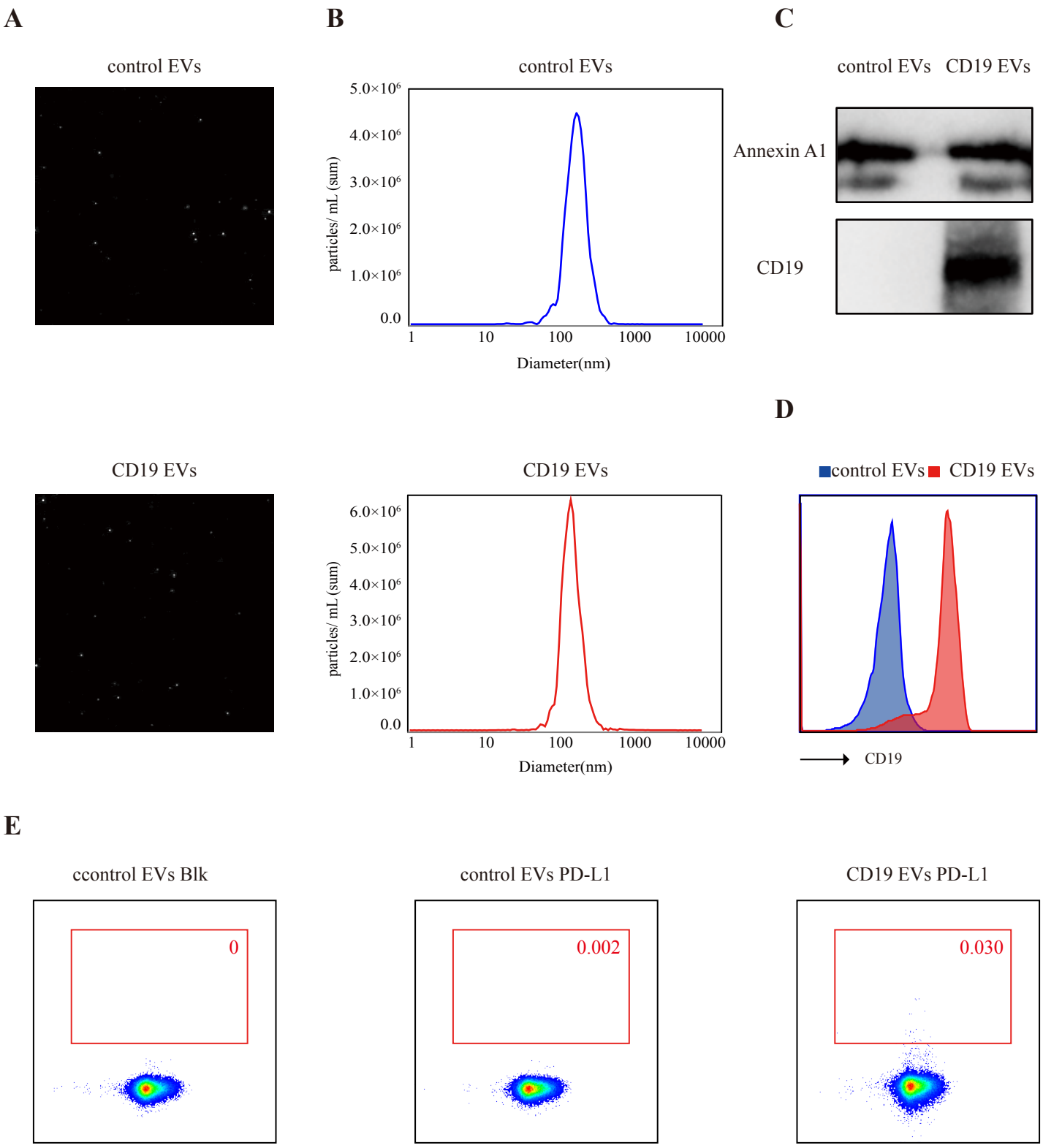
A
control EVs
CD19 EVs
B
control EVs
particles/ mL (sum)
5.0×10⁶
4.0×10⁶
3.0×10⁶
2.0×10⁶
1.0×10⁶
0.0
1
10
100
1000
10000
Diameter(nm)
CD19 EVs
particles/ mL (sum)
6.0×10⁶
5.0×10⁶
4.0×10⁶
3.0×10⁶
2.0×10⁶
1.0×10⁶
0.0
1
10
100
1000
10000
Diameter(nm)
C
control EVs
CD19 EVs
Annexin A1
CD19
D
control EVs
CD19 EVs
CD19
E
ccontrol EVs Blk
0
control EVs PD-L1
0.002
CD19 EVs PD-L1
0.030

Figure S2

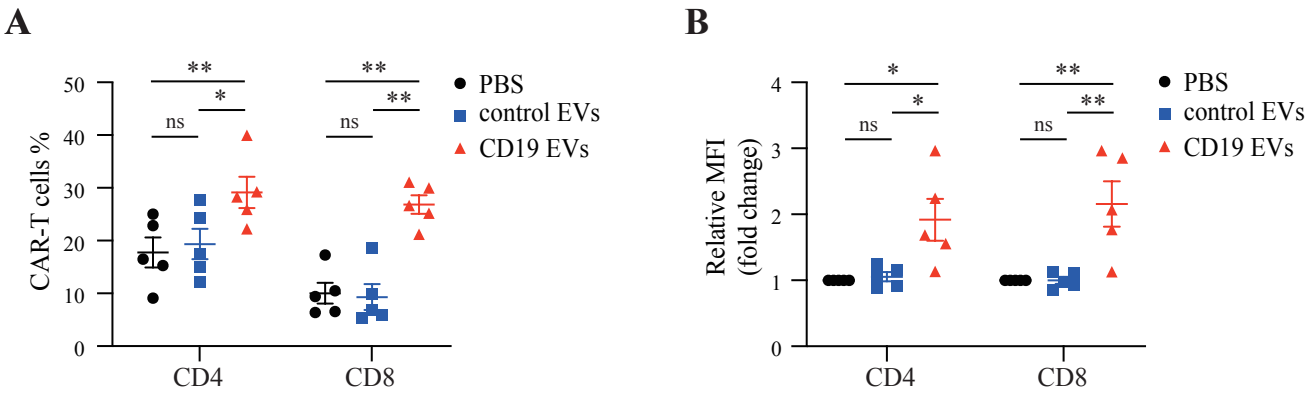
A
B
CAR-T cells %
Relative MFI
(fold change)
PBS
control EVs
CD19 EVs
CD4
CD8
ns
*
**

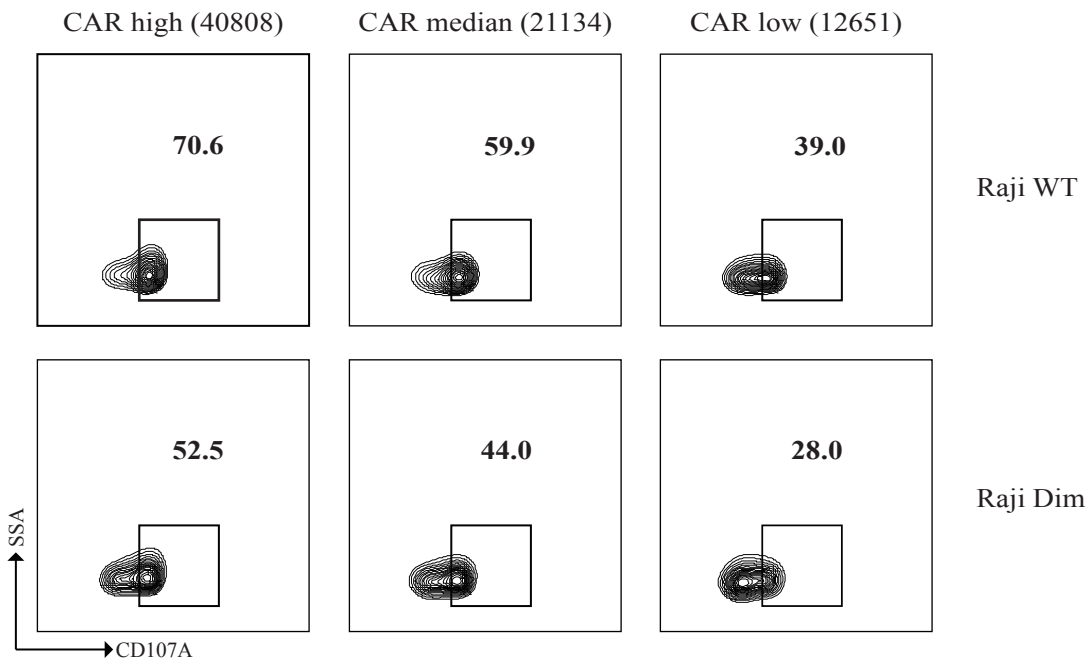
CAR high (40808)
CAR median (21134)
CAR low (12651)
70.6
59.9
39.0
Raji WT
52.5
44.0
28.0
Raji Dim
SSA
CD107A

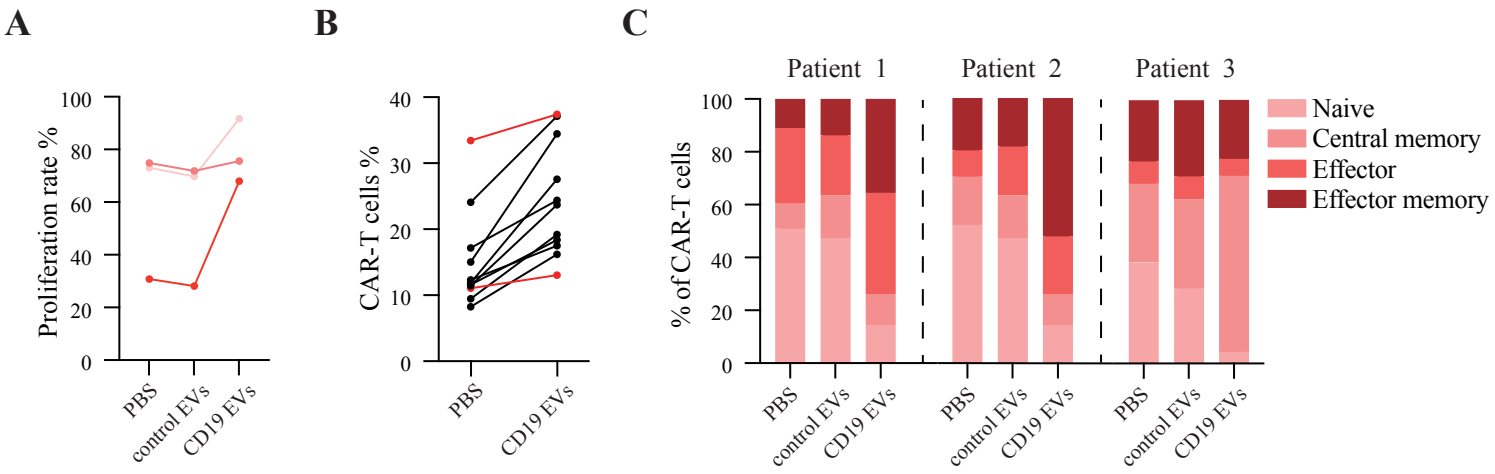
A
Proliferation rate %
100
80
60
40
20
0
PBS
control EVs
CD19 EVs
B
CAR-T cells %
40
30
20
10
0
PBS
CD19 EVs
C
Patient 1
Patient 2
Patient 3
% of CAR-T cells
100
80
60
40
20
0
PBS
control EVs
CD19 EVs
Naive
Central memory
Effector
Effector memory

Figure S5

A

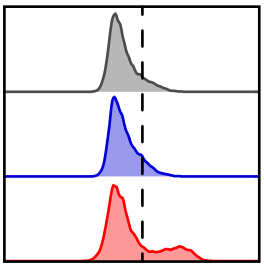

	Input	CART %	CART (MFI)
	CART+PBS	11.0	31367
	CART+control EV	10.5	28358
	CART+CD19 EV	24.8	94021

B

T

CART+PBS

CART+ control EVs

CART+ CD19 EVs

C

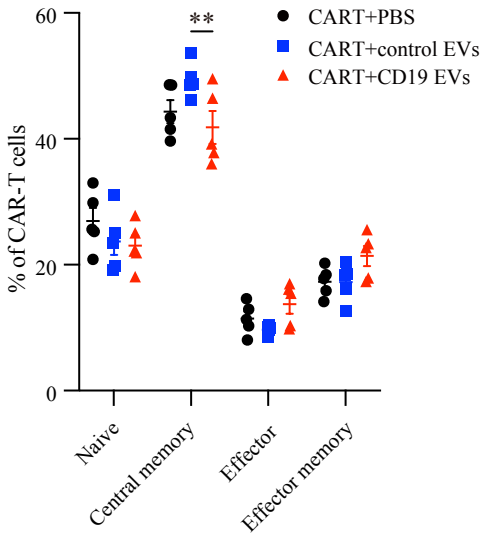

D

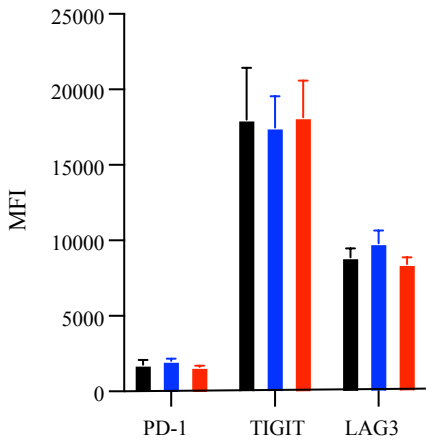

E

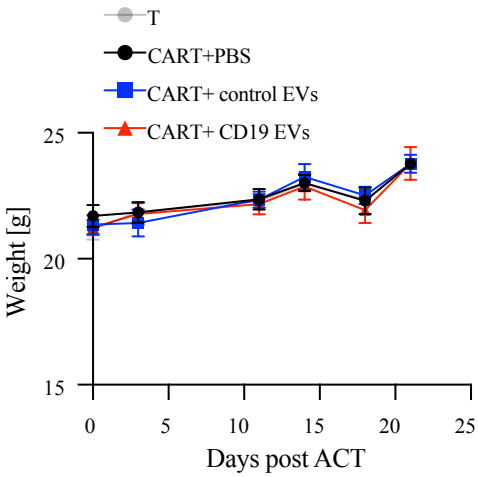

Figure S6

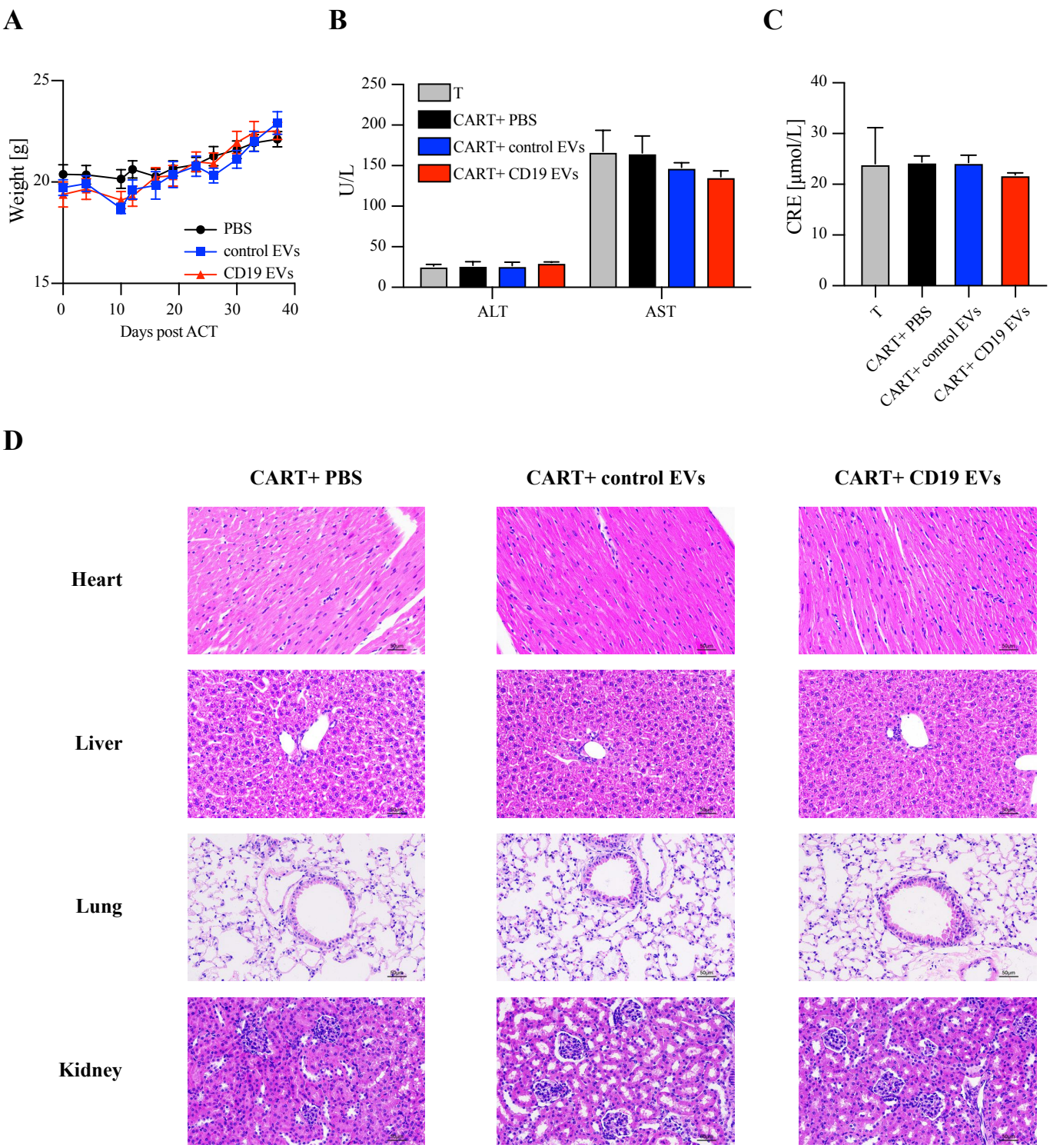
A
Weight [g]
Days post ACT
PBS
control EVs
CD19 EVs
B
U/L
T
CART+ PBS
CART+ control EVs
CART+ CD19 EVs
ALT
AST
C
CRE [μmol/L]
T
CART+ PBS
CART+ control EVs
CART+ CD19 EVs
D
CART+ PBS
CART+ control EVs
CART+ CD19 EVs
Heart
Liver
Lung
Kidney

Supplementary Materials

Supplementary Figure 1 Characterization of control EVs and CD19 EVs. (A, B) NTA was used to examine the Brownian motion and size distribution of EVs. (C) Annexin A1 and CD19 expression of EVs were detected by western blotting. (D) Flow cytometry was performed to detect the expression of CD19 on the surface of EVs. (E) Flow cytometry was performed to detect the expression of PD-L1 on the surface of EVs.

Supplementary Figure 2 CD19 EVs both promote the expansion and CAR expression of CD4+ and CD8+ CAR-T cells. (A) Proportion and (B) CAR MFI of CD4+ and CD8+ CAR-T cells analyzed by flow cytometry after 72 h of co-culture with PBS, control EVs CD19 EVs. ns, not significant; *P <0.05, **P<0.01.

Supplementary Figure 3 Antigen and CAR molecule densities regulate efficacy of CAR-T cells. Flow cytometry detection of CD107a expression in CAR-T cells with varying CAR expression mixed with Raji cells with varying CD19 expression at an effector to target ratio of 1:1.

Supplementary Figure 4 Effect of CD19 EVs on CAR-T cells prepared from patient-derived T cells. (A) CFSE-labeled CAR-T cells were treated with PBS, control EVs and CD19 EVs respectively for 72 h, then proliferation of CAR-T cells was analyzed by flow cytometry. The three lines represent three patients. (B) Black lines represent the patients whose CAR-T cells' proliferation was promoted by CD19 EVs, red lines represent the patients did not achieve the same effect. (C) Subsets was detected using flow cytometry in CAR-T cells after 7 days treatment with PBS, control EVs, and CD19 EVs respectively.

Supplementary Figure 5 CD19 EVs primed CAR-T cells exhibit enhanced anti-tumor activity in vivo. (A) Flow cytometry histograms showing the CAR-T cells primed with PBS, control EVs or CD19 EVs for 72 h before ACT. (B) Photographs of tumor xenografts of tumor mice from each group on day 7 after ACT. (C, D) Subsets and immune checkpoint expression of CAR-T cells was detected by using flow cytometry on day 9 after ACT. (E) Body weight of mice treated with T cells or CAR-T cells (n = 5 animals per group). **P<0.01.

Supplementary Figure 6 Safety of *in vivo* administration of CD19 EVs. (A) Body weight of mice during the time course of the various treatments. (B) Hepatic and (C) Renal function of mice

Information Classification: General

29 determined by chemistry tests. (D) representative images of H&E staining of vital organs on day 8
30 after ACT. Scale bars, 50 μm.